

Polymer Chemistry

Accepted Manuscript



This is an *Accepted Manuscript*, which has been through the Royal Society of Chemistry peer review process and has been accepted for publication.

Accepted Manuscripts are published online shortly after acceptance, before technical editing, formatting and proof reading. Using this free service, authors can make their results available to the community, in citable form, before we publish the edited article. We will replace this *Accepted Manuscript* with the edited and formatted *Advance Article* as soon as it is available.

You can find more information about *Accepted Manuscripts* in the [Information for Authors](#).

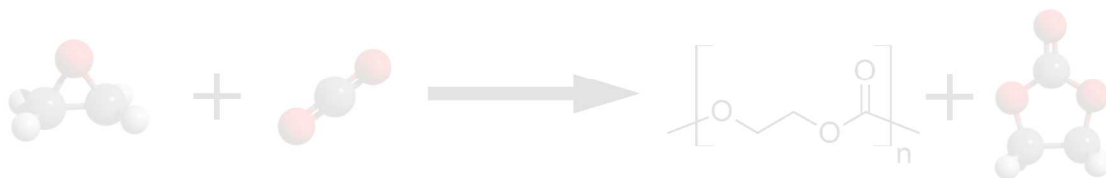
Please note that technical editing may introduce minor changes to the text and/or graphics, which may alter content. The journal's standard [Terms & Conditions](#) and the [Ethical guidelines](#) still apply. In no event shall the Royal Society of Chemistry be held responsible for any errors or omissions in this *Accepted Manuscript* or any consequences arising from the use of any information it contains.

A Concise Review of Computational Studies of the Carbon Dioxide-Epoxyde Copolymerization Reactions

Donald J. Darensbourg and Andrew D. Yeung*

Department of Chemistry, Texas A&M University, College Station, Texas 77843.

** djdarens@mail.chem.tamu.edu*



Computational chemistry:

Thermodynamics of copolymerization
Kinetics of chain growth and degradation
Experimental-computational synergism
Rational catalyst design?

Submitted as a **Review** to *Polymer Chemistry*

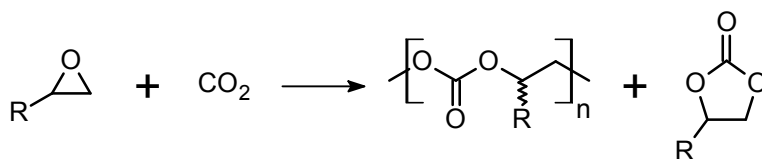
Abstract

The production of polycarbonates from carbon dioxide and epoxides is an important route by which CO₂, a waste product with harmful environmental effects, is converted into useful products. Some of these polymers have been commercialized as binders, adhesives, and coatings; low molecular weight polycarbonate polyols are used to prepare polyurethanes and ABA triblock polymers. Of current interest is poly(glycerol carbonate) that may consume excess glycerol that is generated from biodiesel production. This review surveys the use of computational chemistry toward answering questions pertaining to the CO₂-epoxide copolymerization. Emphasis is placed on the thermodynamics of polymer formation, and the kinetics of polymer growth and degradation.

Introduction

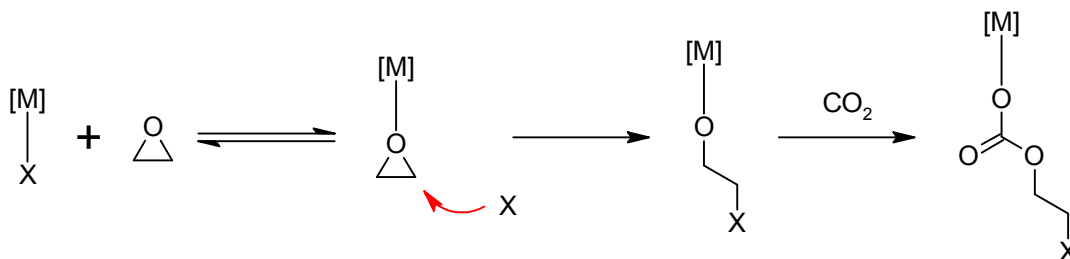
Carbon dioxide is a product of burning carbonaceous fuel, and humans produce it on a grand scale: *ca.* 35 gigatonnes per year. As a greenhouse gas, its increasing concentration in the air is linked to global climate change. There are numerous strategies to reduce carbon dioxide's accumulation, and sequestration in geologic formations is viewed by some as a long-term solution.¹ CO₂ utilization is complementary to such efforts, and incorporation of this gas in useful products provides an opportunity for indirect storage. The production of polycarbonates from CO₂ and epoxides (**Scheme 1**) is one of the focuses of the U.S. Department of Energy's Carbon Storage Program.² As significant energy costs are involved in mechanically compressing CO₂ for use,³ efforts are being made toward the direct use of CO₂ within flue gas.^{4,5}

This copolymerization reaction that was first reported by Inoue and coworkers in 1969⁶ converts an otherwise undesirable waste product into a useful chemical feedstock. Some of these polycarbonates have been commercialized as packaging material and coatings,^{7,8} while low molecular weight poly(propylene carbonate) serves as a drop-in replacement for poly(propylene oxide) used for preparing polyurethanes.⁹ Catalytic systems that produce these polycarbonates have been comprehensively reviewed.¹⁰⁻²⁰

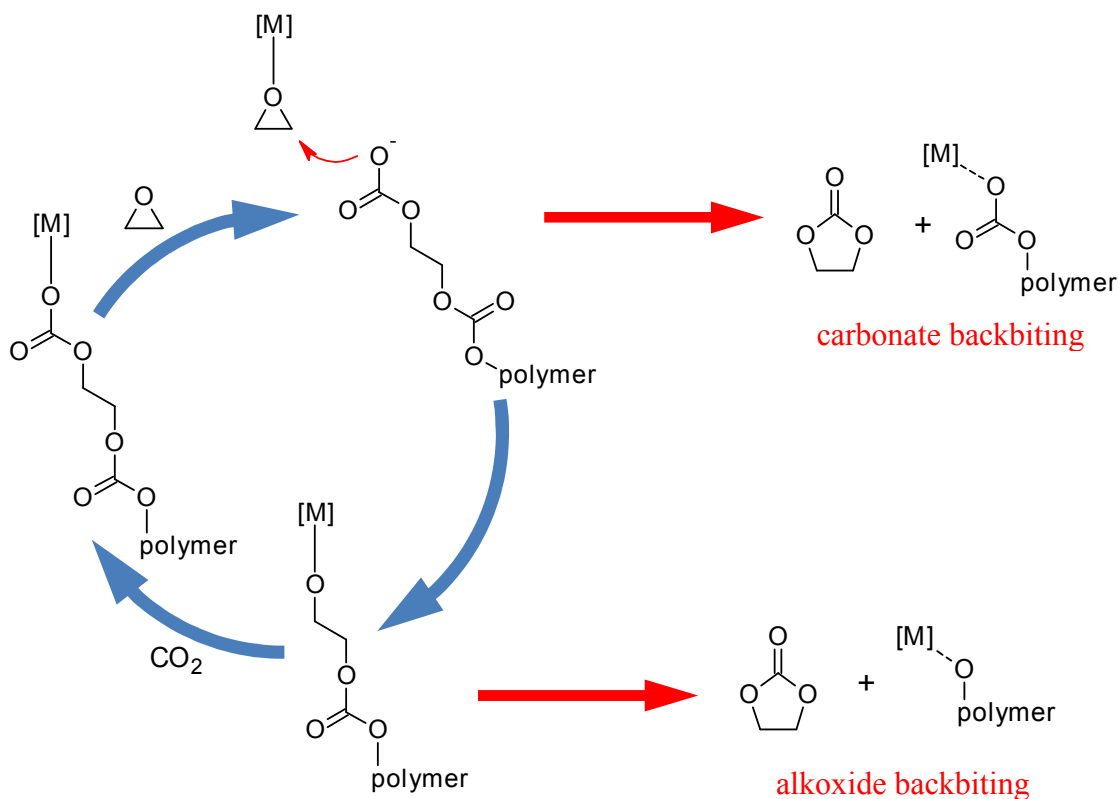


Scheme 1. Reaction between CO₂ and an epoxide to yield the desired copolymer, and cyclic carbonate side-product.

In the general reaction, the polymerization reaction begins when an epoxide co-monomer displaces a metal-bound initiator ligand. The epoxide is activated by a Lewis acidic metal center, and undergoes nucleophilic attack by a suitable initiator, undergoing ring-opening. The alkoxide formed reacts with CO₂ to form a carbonate (**Scheme 2**). This carbonate serves as the nucleophile for subsequent epoxide ring-opening reactions (**Scheme 3**), and the catalytic cycle continues. Along the way, the polymeric carbonate or alkoxide may backbite while metal-bound or metal-free to give the undesired cyclic carbonate.



Scheme 2. The initiation step for the general CO₂-epoxide copolymerization reaction.



Scheme 3. Propagation: Once the initial carbonate is formed, the copolymerization proceeds by successive epoxide ring-opening reactions, followed by CO₂ insertion into the metal-alkoxide bond. The polymeric carbonate (top) or alkoxide (bottom) may undergo backbiting while metal-bound or metal-free to produce, in this instance, the undesired cyclic carbonate side-product.

The first generation of catalysts comprises zinc complexes that trace their lineage to Inoue's diethylzinc-water system such as zinc phenoxides.^{21, 22} Coates *et al.* showed that the zinc-catalyzed reaction was second order in [Zn],²³ leading to the design of dizinc complexes by Coates' and Williams' groups (Figure 1a). Early zinc catalysts were effective for copolymerizing cyclohexene oxide with carbon dioxide, but ineffective for the analogous reaction with propylene oxide. Due to zinc's Lewis acidity, some of these systems catalyzed the epoxide homopolymerization reaction too, resulting in polyether defects within the polycarbonate. The more mature systems are very active, and can provide polyether-free polycarbonate at low CO₂ partial pressures.²⁴ Zinc catalysts are especially well covered in Williams *et al.*'s review.¹⁷

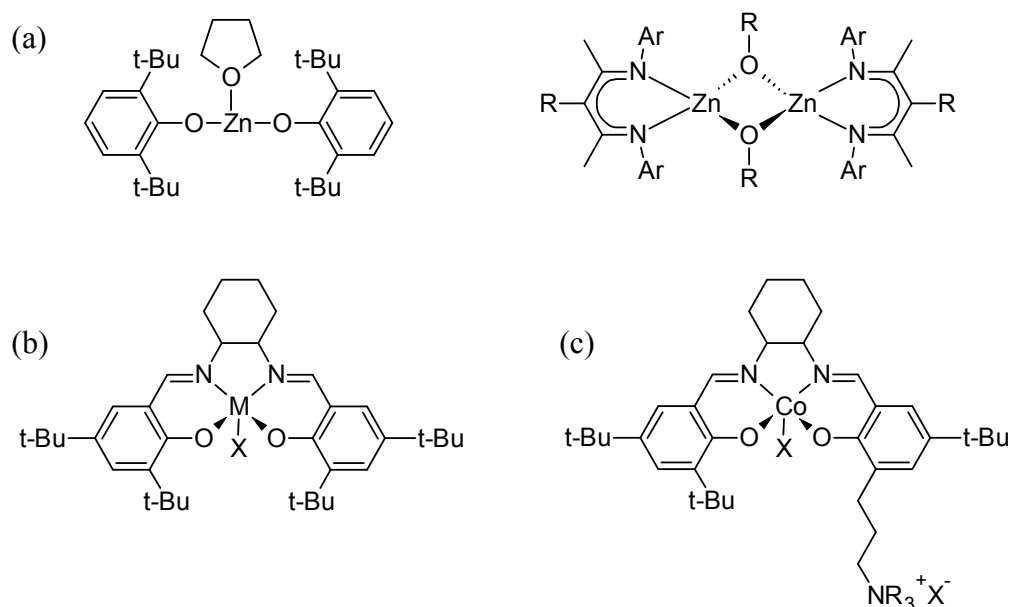


Figure 1. Examples of catalysts for the CO₂-epoxide copolymerization: (a) First generation: a zinc phenoxide catalyst, and a (β-diimine)zinc dizinc catalysts. (b) Second generation (salen)M(III)X catalysts, usually used with cocatalysts. (c) Third generation bifunctional salen-type catalyst that comes with its own cocatalyst.

Subsequently, a second generation of catalysts derived from porphyrin and salen complexes were developed (Figure 1b). In the absence of an onium salt, these catalysts were second order in metal, reminiscent of the well-studied epoxide hydrolysis reaction.²⁵ Coates and coworkers' binap-linked dinuclear cobalt complex was an elegant response to the rate law.²⁶⁻²⁸ However, the addition of cocatalysts converted the square pyramidal complexes to octahedral complexes that were first order in metal. Especially effective cocatalysts in use are the chloride, azide, and dinitrophenolate anions, and the N,N-dimethylaminopyridine (DMAP) and N-methyltriazabicyclodecene (mTBD) neutral amines. These catalysts required modest CO₂ pressures to operate, but yielded copolymers with perfect CO₂ incorporation. Unfortunately, these systems tended to generate cyclic carbonates in addition to the desired polymer. These second generation salen-type catalysts have been comprehensively reviewed by Darensbourg.¹⁵

Third generation cobalt catalysts featuring built-in cocatalysts emerged (Figure 1c). Those bearing quaternary onium cation arms had the added benefit, in that the dissociated anionic polymer chain was kept from being lost to the bulk of the reaction mixture. Proximity allows the polymeric carbonate to quickly return to ring-open the epoxide that displaced it from the metal center. Furthermore, the tethered polymer is prevented from attacking its own carbonyl group, thereby reducing monomer wastage through cyclic carbonate formation. Since they contain their own built-in cocatalyst, they are also named bifunctional catalysts, as opposed to prior binary catalyst/cocatalyst systems. These third generation catalysts are some of the best to date. These third generation cobalt complexes are now able to operate at high temperatures (70-110 °C) that the conventional salen complexes did not survive.^{18, 19}

Now that good general purpose catalysts have been developed, attention has turned toward alternate epoxide monomers like styrene, chloropropylene, and indene oxides (Figure 2).²⁹ Poly(indene carbonate) in particular, has the highest reported T_g (138 °C) for a CO₂-epoxide polycarbonate.^{29, 30} Renewable feedstocks in the form of limonene oxide have been tried too.³¹ Increasing attention is being given toward synthesizing polycarbonate polyols as precursors for ABA-type triblock polymers; poly(propylene carbonate), 43 % CO₂ by weight, is a drop-in replacement for poly(propylene oxide) in the production of polyurethane that has been commercialized by Bayer as *polyether polycarbonate polyols*.⁹ Of current interest are glycerol carbonates^{32, 33} and polycarbonates^{34, 35} ultimately derived from glycerol and CO₂. Such carbonates represent the conversion of two burdensome waste streams into useful materials.

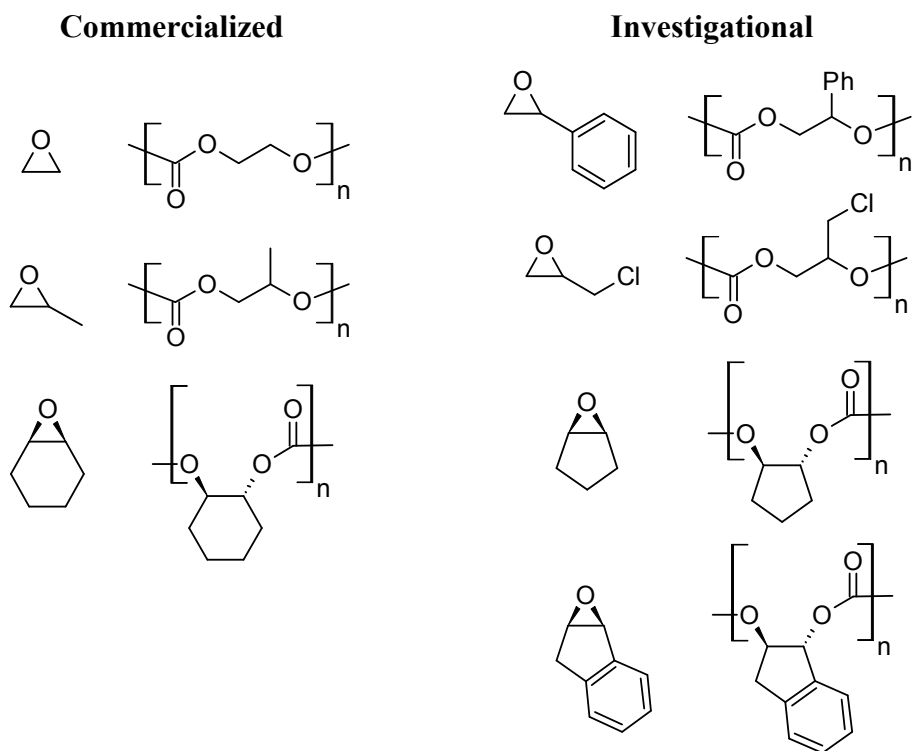


Figure 2. Polycarbonates and their corresponding epoxide precursors. Commercialized (top-bottom): Poly(propylene carbonate), poly(cyclohexene carbonate). Investigational (top-bottom): Poly(styrene carbonate), poly(chloropropylene carbonate), poly(cyclopentene oxide), and poly(indene carbonate).

While much of the current mechanistic understanding of these polycarbonate-forming reactions has been derived from experimental work, the use of computational methods is increasingly popular for solving chemistry problems. The judicious use of computational chemistry can reduce the amount of experimental work to be done, leading to the use of fewer expensive reagents and the generation of less waste. Significantly, computational chemistry allows the chemist to consider elementary reactions separate from other competing reactions. In contrast, many kinetics experiments are unable to distinguish the effects of multiple pathways.

Morokuma and coworkers³⁶ were the first to examine the CO₂-epoxide copolymerization using computational chemistry in 2002. Much has transpired since, though no survey of these computational studies has been performed. Herein, we explore the use of quantum mechanical

methods toward understanding the CO₂-epoxide copolymerization. Outside the scope of this work, reviews of computational methods applied toward utilizing CO₂,^{37, 38} and of the computational prediction of other polymer properties³⁹ are available.

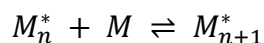
Thermodynamics of polymer formation

Polymerization processes involve the agglomeration of small monomeric units, resulting in the formation of a large macromolecule, with a concomitant decrease in the system's entropy. Axiomatically, polymerization is favored at low temperature, whereas depolymerization is favored at high temperature. ΔS is normally negative, making the entropic $-T\Delta S$ component for the expression of Gibb's free energy ($\Delta G = \Delta H - T \Delta S$) positive. At relatively high temperatures, $-T\Delta S$ may be sufficiently positive that the overall reaction is no longer exergonic. The temperature at which $\Delta G = 0$ is known as the ceiling temperature, T_c , and we can define $T_c = \frac{\Delta H}{\Delta S}$.⁴⁰

The preceding discussion assumes gaseous reactants; phase changes and solvation give rise to drastic changes in enthalpy and entropy.⁴¹ A major exception to our axiom is the ring-opening polymerization of some large, unstrained rings: the loss of translational entropy in individual monomers is countered by the gain of rotational and vibrational entropy present in the flexible polymer chains. These polymers have floor temperatures, T_f , instead of ceiling temperatures.⁴¹

Conventionally, ΔH may be obtained by direct measurement of the heat evolved during a polymerization reaction. It may also be found by calorimetry: samples of polymer and monomer are burned, and the heat evolved is recorded. The difference between the two would represent the enthalpy of polymerization. ΔS may be calculated from the standard entropies of monomer and polymer. These standard entropies are themselves calculated by $S(T) = \int_0^T \frac{C_p}{T} dt$, where C_p is the experimental heat capacity of either at constant pressure.⁴²

In the case of equilibrium reactions, enthalpies and entropies can also be extrapolated by Dainton's equation.⁴³ In the model system reversible addition of a monomer unit, M , to a growing polymer chain, M_n^* , leads to an elongated polymer, M_{n+1}^* :



Since M_n^* and M_{n+1}^* are equivalent, the equilibrium constant, K , can be simplified:

$$K = \frac{[M_{n+1}^*]}{[M_n^*][M]} = \frac{1}{[M]}$$

The Gibbs free energy of reaction is the standard free energy of reaction, corrected with the reaction quotient, Q :

$$\Delta_r G = \Delta_r G^\circ + RT \ln Q = \Delta_r H^\circ - T\Delta_r S^\circ + RT \ln Q$$

At equilibrium, $\Delta_r G = 0$ and $Q = K$:

$$\Delta_r H^\circ - T\Delta_r S^\circ + RT \ln K = 0$$

$$\Delta_r H^\circ - T\Delta_r S^\circ = -RT \ln K$$

Dividing throughout by T , and substituting K for $1/[M]$, we obtain Dainton's equation:

$$R \ln[M] = \frac{\Delta_r H^\circ}{T} - \Delta_r S^\circ$$

Polymerization reactions are run at different temperatures, and the equilibrium concentration of residual monomer is thereafter measured. Plotting $\ln [M]$ against $1/T$ provides $\Delta_r H^\circ$ and $\Delta_r S^\circ$.

Estimating enthalpies of polymerization

One of the oldest methods to calculate enthalpies of polymerization is to use tabulated bond dissociation energies,^{44, 45} be they experimental or theoretical figures. A more sophisticated approach is the Benson and Buss' group additivity method that compensates for the effects of neighboring groups.⁴⁶⁻⁴⁸ Miller *et al.* have demonstrated both approaches for poly(ethylene) and for the ethylene-carbon dioxide copolymer.⁴⁹

Computational chemistry can be used to calculate the enthalpies of monomer vs. oligomer directly. Enthalpies of polymerization are obtained as the enthalpy of chain extension:

$$\Delta H(\text{polymerization}) = \Delta H((n+1)\text{-mer}) - \Delta H(n\text{-mer}) - \Delta H(\text{monomer})$$

This oligomer approach requires the ends of the model polymer to be defined. Hydrogen is the conventional choice, even though hydrogen-capped oligomers are not observed in the actual polymerization processes. This process should in principle be repeated until convergence,⁴⁹⁻⁵² but intramolecular hydrogen bonding may complicate matters. Some workers have chosen to only consider the 1-mer to 2-mer reaction, as the 2-mer is short enough to avoid this problem. They too found the iterative approach for well-behaved polycarbonates superfluous, the 1-mer to 2-mer reaction enthalpy being within 0.1 kcal/mol of the average of several iterations.⁵⁰ Of course, the rate of convergence may differ for other systems, such as for polyacetylenes with extended π systems that Brothers *et al.* has reported.⁵¹

We may consider polymers to be infinitely repeating linear chains, periodic boundary conditions having been applied. In so doing, the chain-end approximations are obviated and complications due to intramolecular bonding are avoided. Additionally, fewer computational resources are needed for modeling a small repeat unit than for a relatively large oligomer. At first glance, the enthalpy of polymerization may simply be calculated:

$$\Delta H(\text{polymerization}) = \Delta H(\text{repeat unit}) - \Delta H(\text{monomer})$$

Brothers *et al.* point out that vibrational analysis of a single repeat unit is inadequate, as vibrations in the whole polymer that are out of phase within a small repeat unit are not taken into account. As a result, supercells (containing more than one repeat unit) are used iteratively to achieve convergence.⁵¹

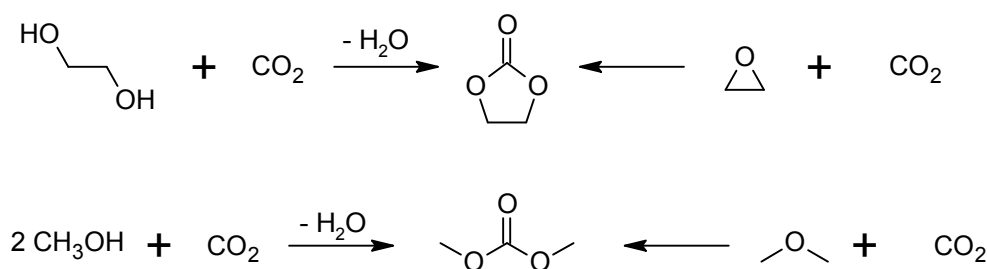
While useful fiction, a real polymer is not an oligomer, nor is it an infinitely long polymer. Even sterically-unencumbered poly(ethylene) is not infinitely long, and linear alkanes of increasing length eventually favor hairpin structures to take advantage of favorable intramolecular van der Waals interactions.⁵³⁻⁵⁵

Benchmarking various computational methods

To the best of our knowledge, only two articles have discussed the thermodynamics of the CO₂-epoxide copolymerization. Both compared polymer vs. cyclic carbonate formation, and both groups investigated polymer formation via the oligomeric approach. In the 2011 article,⁵⁶ the authors compared BP86, m06-l, m06, and m06-2X (in conjunction with electronic energies with

the results of high level CCSD(T)/def-TZVPP calculations, and concluded that no one functional reproduced the high level *ab initio* results perfectly. High accuracy thermochemistry was not a stated goal. Enthalpies of copolymerization vs. cyclic carbonate formation were obtained using BP86/SV(P).

In a later article,⁵⁰ the “chemically accurate” composite CBS-4M method was declared the best after an extensive benchmarking study. Semi-empirical PM6,⁵⁷ DFT, *ab initio*, and composite calculations were carried out to determine the enthalpies for the reactions in Scheme 4, and they showed that the composite methods yielded the “chemical accuracy” (± 1 kcal/mol) promised (Table 1). These composite methods include several *ab initio* calculations that attempt to approximate the “truth” represented by a full configuration interaction calculation using an infinitely large basis set. The Complete Basis Set family achieves this approximation by extrapolation, whereas the Gaussian-n family does so by additive corrections. Unlike *ab initio* calculations, DFT results may not be systematically improved.⁵⁸ CBS-4M was chosen for its ability to handle large oligomers.



Scheme 4. Reactions considered for the benchmarking study in reference 50 (Table 1). The carbonates included in the test set were ethylene, propylene, and butylene cyclic carbonates, and dimethyl, diethyl, and diphenyl acyclic carbonates.

Table 1. Results of the benchmarking study in **Scheme 4**.⁵⁰ Deviations (kcal/mol) = calculated enthalpy – experimental gas phase enthalpy (from NIST).

	Mean signed deviation	Mean unsigned deviation	Root mean squared deviation
NIST error		1.9	2.4
B3LYP/6-311G(2df,p)	4.9	4.9	5.3
TPSSTPSS/6-311G(2df,p)	4.9	4.9	5.3
mPWPW91/6-311G(2df,p)	4.8	4.8	5.2
m06-2X/6-311G(2df,p)	-1.2	2.1	2.5
MP2/6-311G(3d2f,p)	3.5	3.5	3.8
CCSD/6-311G(3d2f,p)	0.7	1.6	2.0
CBS-4M	0.1	0.8	1.1
CBS-QB3	-0.3	0.7	0.8
G3MP2	1.2	1.2	1.8
G4	0.7	0.9	1.1

To supplement the reliable but computationally intensive CBS-4M method, the authors sought a less computationally demanding method to calculate “ballpark” enthalpies of polymerization. They examined the use of PM6 for this purpose because this method requires minimal computational resources. The use of periodic boundary conditions was also of interest, because smaller systems might stand in for large oligomers. They wanted to make use of PM6 for this purpose, because MOPAC directly reports enthalpies of formation, whereas Gaussian 09 is generally unable to do so for PBC calculations. Initial results were promising, but PM6 was ultimately found to be unsuitable. Compared with the experiment,^{59, 60} PM6 underestimates carbon dioxide’s enthalpy of formation by 9.3 kcal/mol, whereas it overestimated dimethyl, diethyl, and diphenyl carbonates’ enthalpies of formation by 6.5-11.5 kcal/mol. This unintended cancellation of error led to PM6’s seemingly excellent performance in the benchmarking study.⁵⁷

The CO₂-epoxide copolymerization

In both articles that discuss the CO₂-epoxide copolymerization, polymer formation was studied via the oligomeric approach. Rieger *et al.* reported enthalpies obtained by density functional theory (BP86/SV(P)),⁵⁶ whereas Darensbourg and Yeung used the “chemically accurate” composite CBS-4M method.⁵⁰ Of passing relevance is the article by Miller *et al.* that modeled the copolymerization of ethylene with carbon dioxide using the oligomeric approach, with

enthalpies obtained by DFT (B3LYP/6-31G(d')).⁶¹ The enthalpies of polycarbonate formation are compared in Table 2.

Table 2. Enthalpies of the reactions to produce polymers and cyclic carbonates.

	Polymer			Lit.	Cyclic carbonate			NIST ^{59, 60}
	CBS-4M ⁵⁰	B3LYP/6-31G(d') ⁵⁰	BP86/SV(P) ⁵⁶		CBS-4M ⁵⁰	B3LYP/6-31G(d') ^c	BP86/SV(P) ⁵⁶	
EC	-21.2	-21.5	-17.8	-20.8 ^a	-15.1	-15.4	-15.0	-15.2
PC	-21.2	-20.1	-13.6		-15.7	-15.1	-14.7	-16.1
CHC ^b	-22.6	-17.0	-17.4		-16.7	-14.0	-14.5	

^a $\Delta H_{\text{poly}} = -124.5$ kJ/mol by calorimetry. The gas phase enthalpy of polymerization was estimated by subtracting -37.5 kJ/mol,^{59, 60} the enthalpy of vaporization of dimethyl carbonate (representing approximately one repeat unit). ^bTo give the *cis*-cyclic carbonate. ^cNot previously published.

CBS-4M, B3LYP/6-31G(d'), and BP86/SV(P) calculated the enthalpies of cyclic carbonate formation well. For determining enthalpies of polymerization, B3LYP/6-31G(d') agreed well with CBS-4M, as with the single literature data point. The BP86/SV(P) level of theory appeared to have more significant deviations. Despite B3LYP/6-31G(d')'s general agreement with CBS-4M, the authors do not recommend its use where accurate thermochemistries desired, because it (and other functionals tested) experienced significant sensitivity to the basis set chosen.⁵⁰

The authors continue to tabulate both enthalpies and free energies of polymer growth vs. cyclic carbonate formation, and their latest table is reproduced below (Table 3).^{50, 62} These free energies include vibrational corrections obtained. Entropies obtained this way are quite sensitive to low vibrational frequencies,⁴² but the authors expect that most errors are systemic, and that calculated free energies are at least qualitatively correct.

Table 3. Thermodynamics of polymer vs. cyclic carbonate formation.^{50, 62}

	Enthalpy (kcal/mol)		Free Energy (kcal/mol)	
	Polymer	Cyclic carbonate	Polymer	Cyclic carbonate
Ethylene carbonate	-21.2	-15.1	-0.4	-3.8
Propylene carbonate	-21.2	-15.7	0.5	-4.2
Chloropropylene carbonate	-22.1	-13.8	0.1	-2.5
Styrene carbonate [†]	-22.8	-14.8	-0.8	-3.4
Cyclopentene carbonate*	-15.8	-14.5	7.1	-5.8
Indene carbonate*	-21.1	-18.2	1.5	-6.6
Cyclohexene carbonate*	-22.6	-16.7	3.4	-4.6
Trimethylene carbonate	-23.1	-11.7	-2.6	-0.8
1,2-Glycerol carbonate	-21.3	-16.2	0.6	-4.3
1,2-Glycerol carbonate, methyl ether	-22.1	-15.3	0.0	-3.9
1,3-Glycerol carbonate	-22.3	-9.0	-0.5	1.7
1,3-Glycerol carbonate, methyl ether	-20.9	-8.2	0.7	2.8

Average of 4 iterations unless noted. * Calculated from 1-mer + CO₂ + epoxide → 2-mer. † Average of 3 iterations (until 4-mer).

Polymer formation is more exothermic but less exergonic than cyclic carbonate formation for all examples, except for trimethylene carbonate obtained from CO₂ and oxetane. These figures explain why trimethylene carbonate is quantitatively converted to the polymer,⁶³ whereas five-membered cyclic carbonates do so with concomitant decarboxylation (gain of entropy).⁶⁴⁻⁶⁶ Pendant groups on aliphatic polycarbonates rotate out of the way, even for poly(head-to-head propylene carbonate), so they do not contribute to intramolecular steric repulsion. On the other hand, poly(cyclopentene carbonate) experiences significant intrachain repulsion, resulting in its lowered enthalpy of polymerization. Happily, the poor exothermicity of the CO₂-cyclopentene oxide copolymerization gives rise to a polymer that is easily recycled to the constituent monomers.^{67, 68}

Kinetics of chain growth

The kinetics of the CO₂-epoxide copolymerization was first studied computationally by Morokuma *et al.*³⁶ Computational analysis has been done for other first generation zinc catalysts, and for the second generation cobalt and chromium systems supported by salen ligands. Also of

interest to workers in this field is similar work done for the ring-opening polymerization of lactide⁶⁹⁻⁷¹ and caprolactone.⁷²

Zinc-catalyzed routes

The first computational study of the CO₂-epoxide copolymerization was reported by Morokuma *et al.* in 2002.³⁶ It was performed on Coates' (β -diiminato)zinc complex (Figure 3), and the monomeric form was presumed. A two-layer ONIOM approach was used, with the low layer represented by the semi-empirical PM3 method, and the catalytic center calculated with the B3LYP functional and the LANL2DZ and LANL2DZ(d) (added polarization functions) basis sets (denoted PM3:B3LYP/LANL2DZ and PM3:B3LYP/LANL2DZ(d)).

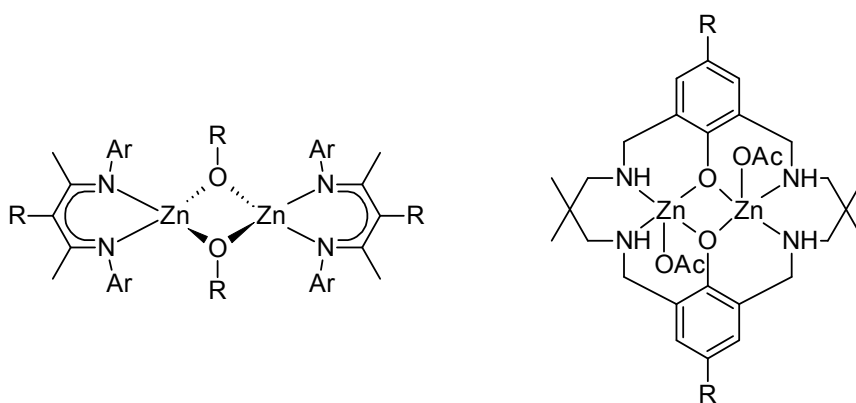


Figure 3. General structures of the bis(β -diiminato) (left) and the Robson-type (right) dizinc catalysts.

A plausible sequence of reactions for the CO₂-epoxide copolymerization was mapped out, ethylene oxide serving as the prototypical epoxide. In this sequence, carbon dioxide weakly coordinates to the coordinatively unsaturated zinc-bound polymeric alkoxide (trigonal planar, 16 electron) via one of its oxygen atoms (O-Zn = 2.497 Å, binding energy = 1.7 kcal/mol) according to PM3:B3LYP/LANL2DZ, while no analogous structure was found at the PM3:B3LYP/LANL2DZ(d) level of theory. The authors found CO₂ insertion into the Zn-methoxide to be barrierless. Subsequently, epoxide coordinates to the catalytic center. The zinc-bound polymeric carbonate (represented by methyl carbonate) attacks a methylene carbon of the

tethered ethylene oxide, but it is unable to approach from the back side like in an S_N2 reaction. As a result, this transformation is asynchronous, and ring-opening of the epoxide occurs before the O-C bond forms. At the transition state, the breaking epoxide O-C bond is longer than the nascent O(carbonate)-C(epoxide) bond. The rate limiting step for this reaction is the last: ring-opening ethylene oxide by the polymeric carbonate, with a very high free energy barrier of 36.4 kcal/mol.

The authors attributed cyclohexene oxide's polymerizability vs. ethylene oxide's lack thereof to relief of ring strain in the bicyclic system. In support, they showed that hydration of cyclohexene oxide was ca. 40 kcal/mol more exoergic than the hydration of ethylene oxide. Recalculated at the CBS-4M level of theory, we find that hydration to *trans*-eq-cyclohexan-1,2-diol is exothermic by 23.0 kcal/mol, comparable to that of -22.3 to -23.9 kcal/mol for ethylene oxide. In contrast, hydration of *trans*-cyclohexene oxide to give *cis*-cyclohexan-1,2-diol is exothermic by 62.3 kcal/mol. Later studies also indicate that the enthalpies for aliphatic and alicyclic epoxides to copolymerize with carbon dioxide are similar.^{50, 56} Morokuma *et al.* might have considered *trans*-cyclohexene oxide instead of the *cis* isomer used for copolymerization with carbon dioxide. This point may be moot because the (BDI)zinc system has since been found to operate via a bimetallic mechanism.²³

In the following computational report,⁵⁶ propylene and cyclohexene oxides were found to behave similarly in principle. The reason propylene oxide does not copolymerize with CO_2 is that the zinc-catalyzed carbonate-backbiting reaction successfully competes with the zinc-catalyzed enchainment reaction (epoxide ring-opening is the rate-determining step; $\Delta G^\ddagger = 23.7$ and 22.6 kcal/mol, respectively). Since propylene carbonate is unable to undergo ring-opening polymerization, it serves as the thermodynamic sink of the system, and any poly(propylene carbonate) that manages to form is eventually destroyed. Cyclohexene oxide avoids this fate by having a higher free energy barrier for zinc-catalyzed carbonate backbiting than zinc-catalyzed polymer growth ($\Delta G^\ddagger = 26.4$ and 18.6 kcal/mol, respectively). The authors expanded upon this work by designing a dinuclear zinc complex that solves the "entropy problem" in that at high temperatures, the monomeric zinc complexes are less likely to aggregate to provide the required catalytic activity.⁷³ This catalyst is flexible enough to accommodate varying Zn-Zn distances along the reaction coordinate (4.50-5.66 Å). Unusually, the rate-determining step is CO_2

insertion. Where CO_2 pressure were increased, this catalyst system's rate-determining step switches from CO_2 insertion to epoxide ring-opening. This study is noteworthy for demonstrating effects of pressure on the calculated reaction profile.

Rzepa, Williams and coworkers subsequently performed a computational-experimental investigation.⁷⁴ They chose to use the dispersion-corrected $\omega\text{B97X-D}$ functional⁷⁵ in conjunction with the double-zeta 6-31G(d) basis set; geometries were essentially the same when a larger basis set was used. They found that the Robson-type dizinc complex (Figure 3) favors a bowl conformation over an "S" conformation by 15.3 kcal/mol, and that only one of the acetate ligands initiates a single polymer chain. Experimental infrared spectra were compared with the predicted spectra of the zinc complexes after one CHO ring-opening reaction, and after that alkoxide complex underwent carboxylation. These spectra were in general agreement.

In this catalytic cycle, both zinc centers work cooperatively to enable CHO and CO_2 to copolymerize. The epoxide coordinates to one zinc center, and it undergoes ring-opening by the acetate ligand on the other zinc center. Two plausible scenarios exist: the acetate may attack via the zinc-coordinated oxygen atom, or it may attack via the uncoordinated carbonyl oxygen with concomitant cleavage of the zinc-oxygen bond. Unsurprisingly, the second route is more accessible than the first ($\Delta G^\ddagger = 24.3$ vs. 41.9 kcal/mol). The supporting acetate bridge assists by facilitating electron flow between the two otherwise-unconnected zinc centers (Figure 4), confirmed by appropriate changes in the acetate Zn-O bond lengths. In the next step, the zinc-bound alkoxide attacks CO_2 to generate a zwitterionic carbonate. The carbonate coordinates to the adjacent zinc center in a separate step. Eventually, the carbonate attacks another zinc-bound cyclohexene oxide ligand, preferentially via the free carbonate oxygen. In agreement with previous reports,^{36, 56} this step is rate-determining. The theoretical and experimental free energies were in excellent agreement too (25.7 vs. 23.5 kcal/mol at 353 K).

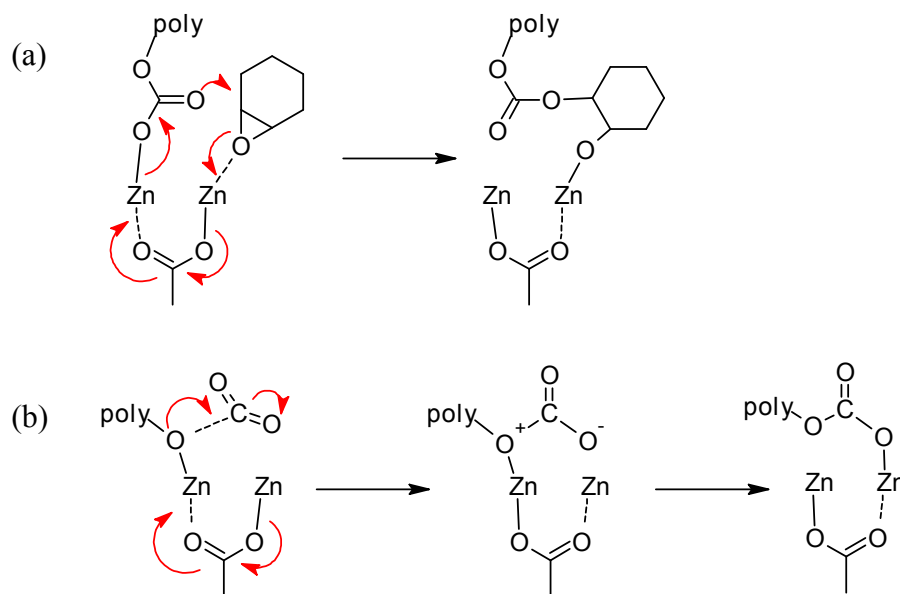


Figure 4. The bridging acetate ligand facilitates the flow of electrons according to Rzepa, Williams, and coworkers: (a) Ring-opening of the zinc-bound cyclohexene oxide ligand via the free carbonate oxygen. (b) The zinc-bound alkoxide attacks a carbon dioxide molecule that is not pre-coordinated.

Side reactions were examined too. Sequential epoxide ring-opening that leads to polyether defects had a very high free energy barrier ($\Delta G^\ddagger = 39.3$ kcal/mol), despite being exergonic. Conversely, sequential CO_2 enchainment is endergonic and unfavored ($\Delta G = 22.8$ kcal/mol), even though its elementary steps had modest barriers.

The defining difference between the (BDI)zinc and subsequent (salen)M(III)X (X = cocatalyst) systems is that the zinc catalyst is coordinatively unsaturated, whereas the octahedral salen complexes do not have vacant coordination sites. That is to say, the polymeric carbonate ring-opens the epoxide while both moieties are zinc-bound, whereas epoxide displaces the polymeric carbonate for at least the cobalt(III) and chromium(III) complexes, and the free polymeric carbonate ring-opens the activated epoxide ligand in an $\text{S}_{\text{N}}2$ -like fashion. These details are discussed in the next section.

Liu and coworkers studied different possible pathways of ZnEt_2 -glycerine and ZnEt_2 -glycerine- YCl_3 catalyst systems using DFT.⁷⁶ Consistent with the literature, the rate-determining step was

the ring-opening of the epoxide co-monomer. The former system was found to have lowest free energy barriers when a dizinc mechanism was considered. Epoxide ring-opening had the lowest barrier when the zinc center that activates it had the most positive NBO charge. This correlation inspired the addition of $(Cl_3CO_2)_3Y$ as a Lewis acid cocatalyst. The dizinc-yttrium complex successfully reduced the free energy barriers for epoxide ring-opening from 32.2 to 27.1 kcal/mol. Experimentally, addition of $(Cl_3CO_2)_3Y$ caused the catalyst to be thrice as active.

Besides these molecular catalysts, Luinstra and Molnar mentioned some preliminary work⁷⁷ on the heterogeneous zinc glutarate catalyst.⁷⁸ They modeled the ethylene oxide homopolymerization reaction on the zinc glutarate surface using Car-Parrinello molecular dynamics. Like the dizinc mechanisms for molecular catalysts, one zinc center activates an ethylene oxide molecule for nucleophilic attack by a polymeric alkoxide tethered to an adjacent zinc center; the propylene-CO₂ copolymerization is expected to proceed in a similar fashion.

Cobalt(III) and chromium(III)-catalyzed routes

Unlike the zinc-catalyzed routes, closed-shell singlet electronic states may not be assumed for the rest of the first transition series. Prior to an in-depth discussion on the CO₂-epoxide copolymerization, we note that the mechanism for epoxide hydrolysis has parallels with the epoxide ring-opening step of the CO₂-epoxide reaction (**Scheme 2** and **Scheme 3**). The nature of the hydrolysis reaction was clarified by experimental^{25, 79} and theoretical studies.^{80, 81}

In the Jacobsen article, (salen)Co(III)-bound hydroxide is the nucleophile that ring-opens the similarly coordinated epoxide. The steric bulk of the both salen ligands and the manner in which they are “stepped”, controlled by the chiral cyclohexylene backbone,⁸² enhance differences in reactivity between the two epoxide substrates. Differences in electronic energy between the “matched” and “mismatched” systems were determined at the B3LYP/6-31G(d) level of theory to be 2-4 kcal/mol. Differences were more prominent (6-9 kcal/mol) at the m06-L/6-31+G(d) level that places more emphasis on weak dispersion interactions. The authors also acknowledged that the triplet (spin-unpaired) octahedral [Co]-OH complex’s hydroxy ligand may be more labile (due to occupation of the anti-bonding $d(x^2-y^2)$ and $d(z^2)$ orbitals, compared with for a low-spin d_6 complex), but found that nucleophilic attack by the hydroxy ligand occurs while the ligand is

still firmly bound to the cobalt center. This indicates that the hydroxy ligand's nucleophilicity while cobalt-bound determines its reactivity more than its lability.

At about the same time, Coates, Cavallo, and coworkers did a computational-experimental study of the epoxide homopolymerization using Coates' binap-linked bimetallic catalyst (Figure 5). They found that methine attack (leading to a head-head mis-insertion) and ring-opening of R-propylene oxide by the (R,R,R,R)-dicobalt catalyst were disfavored by ca. 4 kcal/mol of free energy. The authors were able to account for the system's good stereo- and region-selective homopolymerization (*rac*-propylene oxide yields isotactic poly(propylene oxide) with > 99 % regioselectivity). A bimetallic mechanism has also been described for the homopolymerization of propylene oxide by uranyl catalysts.⁸³

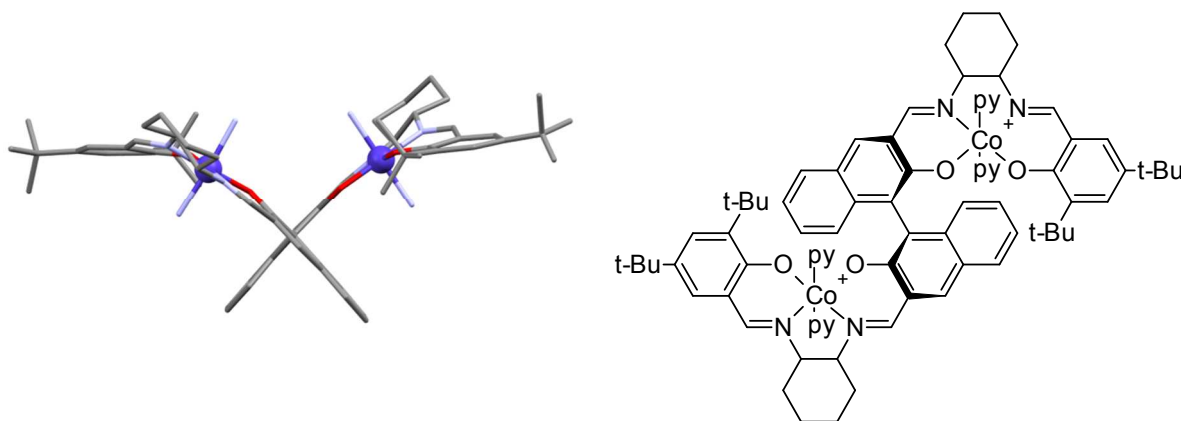


Figure 5. Left: X-ray crystal structure of the binap-linked dicobalt catalyst,²⁸ showing the catalytic groove (Co-Co = 6.937 Å). Hydrogen atoms, counterions, and solvent not shown; free uncoordinated pyridine ligands have been reduced to nitrogen atoms. Dark blue = cobalt; gray = carbon; red = oxygen; light blue = nitrogen. Right: A two-dimensional representation of this complex, py = pyridine.

Also of importance to the CO₂-epoxide copolymerization, Curet-Arana and coworkers examined plausible interactions between carbon dioxide and metal-salen complexes, and concluded that the former does not bind directly to the metal-salen complex (endothermic by ca. 50 kcal/mol).⁸⁴

This is consistent with our understanding that CO₂ insertion does not involve the metal center, based on experimental kinetics studies.⁸⁵⁻⁹⁰

Preliminaries aside, the first theoretical examination of the CO₂-epoxide copolymerization catalyzed by (salen)M(III) complexes was performed by Luinstra *et al.* in 2005. This older study made use of a minimal salen-like ligand for computational efficiency that was found to give results equivalent to the full salen complex. Several metal(III) complexes were examined, as were chloride, acetate, and N,N-dimethylaminopyridine cocatalysts. Luinstra *et al.* determined that when epoxides bind to square pyramidal (salen)M(III)X complexes, they are activated toward ring-opening to a great degree; $\Delta E^\ddagger = 0.5\text{-}6.9$ kcal/mol (E referring to electronic energy), acetate being the nucleophile. That is to say, epoxide ring-opening has a minimal barrier for reaction.

The following CO₂ insertion reaction has significant electronic energy barriers of 10.3 kcal/mol and 23.7 kcal/mol for octahedral iron(III) and aluminum(III) acetatoethoxide complexes, whereas no such transition state could be found for chromium(III). Instead, one of the salen phenoxide ligands had to de-coordinate ($\Delta E^\ddagger = 23.9$ kcal/mol) in order for the carboxylation to occur, prior to barrierless CO₂ insertion, and phenoxide re-coordination. In contrast, electronic energy barriers for the neutral (salen)M(III) acetatoethoxide complexes to undergo carboxylation were lower, at 10.8 and 9.1 kcal/mol for chromium and aluminum respectively.

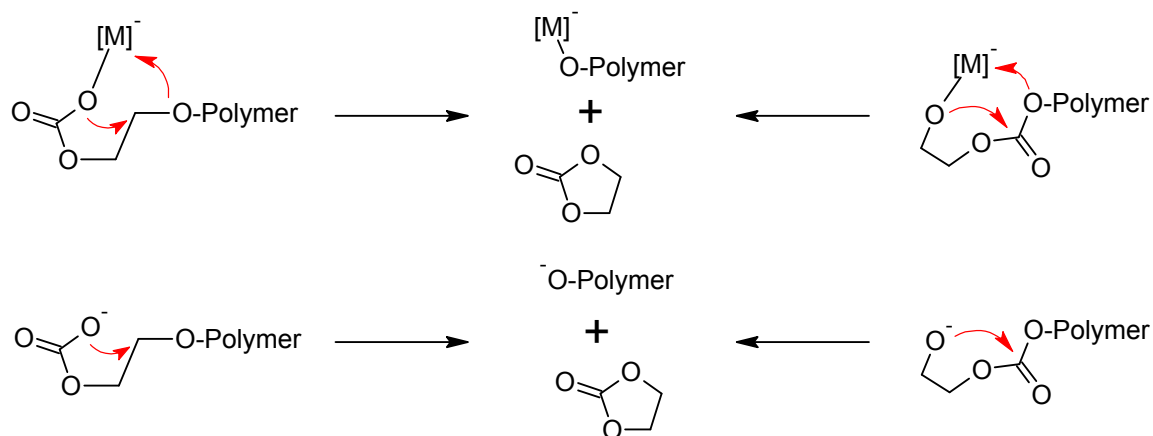
Despite minimal barriers for free acetate to ring-open octahedral metal-bound ethylene oxide molecules, the only low-energy pathway for the ring-opening of the metal-bound epoxide molecule necessitated attack by another metal-bound carbonate ligand. These reactions had barriers of ca. 10 kcal/mol, regardless of the system's spin configuration. The authors acknowledge that vibrational corrections to obtain free energies may change the energy profile of these reactions. With that said, they conclude that at low CO₂ partial pressures, CO₂ insertion is rate-limiting. Additionally, they note that the carbonate ligands dissociate from aluminum complexes more easily than chromium complexes ($\Delta G = 10.7$ vs. 19.1 kcal/mol). After this dissociation, metal-free backbiting can commence, and this helps to explain why aluminum complexes are good for making cyclic carbonates.

Nguyen and Baik studied the formation of cyclic carbonates (the epoxide ring-opening and carboxylation steps are common with the copolymerization reaction) using the B3LYP functional.⁹¹ DMAP serving as the nucleophile, ring-opening [Cr]-bound propylene oxide had a free energy barrier of 23.1 kcal/mol, in contrast with Luinstra's 0.5-6.9 kcal/mol electronic energy barrier. They found that carboxylation was not rate-limiting ($\Delta G^\ddagger = 16.0$ kcal/mol), whereas Luinstra found that CO₂ insertion had the highest barrier ($\Delta E^\ddagger = 23.9$ kcal/mol). The authors were unable to find a bimetallic pathway.

Apart from mapping the peaks and valleys in the energy profile of the copolymerization reaction, we have found an example of computational chemistry standing in for physical measurements. In 2009, Lee *et al.* noted that one of their highly-active cobalt-salen complexes behaved quite unusually. The imine nitrogens on the salen backbone that are usually expected to coordinate to the metal center was not bonded to the metal, two coordination sites having been occupied by dinitrophenolate ligands. In the absence of definitive crystallographic evidence, gas phase DFT calculations were used to support their proposed structure. The unusually coordinated complex was 34 kcal/mol lower in electronic energy to the complex with a "conventional" arrangement, plus two dinitrophenolate ligands. The difference in electronic energy was corrected for electrostatic attraction between the free dinitrophenolate ligands and the quaternary ammonium cations on the salen ligand.⁹² The use of a solvation model would have stabilized the anion better, providing more accurate differences in energy.

Kinetics of backbiting

Efforts to prepare polycarbonates have long been complicated by parallel cyclic carbonate co-product that is thermodynamically favored. In the generally-accepted catalytic cycle, the catalyst-bound polymeric carbonate is displaced by an epoxide unit, before being ring-opened by the displaced carbonate. Cyclic carbonate formation occurs when the free polymeric carbonate (or polymeric alkoxide, under low-CO₂ conditions) backbites upon itself to extrude one unit of cyclic carbonate, leaving behind a shortened polymer chain. The metal-bound polymeric carbonate or alkoxide are less nucleophilic, so they are less susceptible to this degradation reaction (**Scheme 5**). Complete dissociation of the polymeric carbonate has resulted in the design of catalysts bearing tethered onium cations that trap these polymeric carbonates, preventing this deleterious side reaction. These catalysts are some of the most active yet.¹⁸



Scheme 5. The principal paths by which polycarbonates degrade to cyclic carbonates.

Experimentally, the kinetics of these nuisance chromium-bound degradation reactions were measured alongside the target polymerization reaction by *in situ* infrared spectroscopy,^{93, 94} and the metal-free degradation reactions were the focus of a dedicated investigation.⁹⁵ Luinstra, Rieger *et al.* studied the metal-bound and metal-free carbonate backbiting reactions using gas phase BP86/SV(P) geometries, supplemented by BP86/TZVP single point energies.⁹⁶ Ethylene oxide was the prototypical epoxide, and the authors approximated the remainder of the polymer chain with acetate. For the metal-bound degradation reactions, the chromium(III) and aluminum complexes were greatly truncated. The authors concluded that the metal-free carbonate backbiting reaction is the most likely degradation route, while metal-bound carbonate degradation routes are more difficult (Table 4). The authors did not find pathways for metal-bound or metal-free alkoxide backbiting reactions, noting that a polymeric alkoxide is a poor leaving group.

Table 4. Electronic energy barriers (kcal/mol) to carbonate backbiting per reference 96.

Polymeric carbonate bound to	ΔE^\ddagger
[Cr]-OAc	22.7
[Cr]-Cl	21.5
[Cr]-DMAP	31.6
[Al]-Cl	22.2
Metal-free	8.4

The kinetics of metal-free backbiting reactions were obtained independently using the composite CBS-QB3 and CBS-QB3(+).⁵⁰ The authors favor composite methods for their more accurate thermochemistries, and the CBS-QB3 method makes use of B3LYP/6-311G(2d,d,p) geometries that are superior to HF/3-21G geometries used by CBS-4M for these bond-forming and bond-breaking reactions. The authors successfully located transition states for alkoxide-backbiting reactions by the use of added diffuse functions. Martin's modified CBS-QB3(+) method⁹⁷ utilizing B3LYP/6-311+G(2d,d,p) geometries was used for these calculations. Their results are summarized in Table 5.

Table 5. Free energies barriers (kcal/mol) for metal-free backbiting reactions.⁵⁰

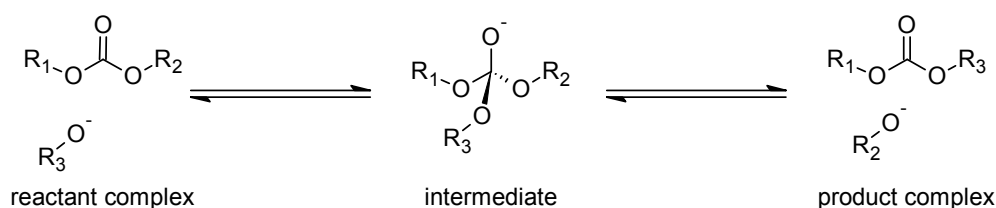
	Carbonate backbiting (methine, methylene attack)	Alkoxide backbiting (lowest barriers)
EC	20.4	11.6
PC	24.0, 18.5	11.8
CIPC	25.5, 19.7	12.4
SC	19.5, 20.2	10.7
<i>cis</i> -CPC ^a	20.3	
<i>trans</i> -CPC ^a		19.9
<i>cis</i> -CHC ^a	25.8	
<i>trans</i> -CHC ^a		14.6

^aCis epoxides generate trans polymers. Carbonate backbiting produces cis-cyclic carbonate due to inversion at the point of substitution, whereas the trans configuration is retained in alkoxide backbiting.

In contrast to Luinstra, Rieger, *et al.*'s assertion, the metal-free carbonate backbiting has a higher free energy barrier (20-25 kcal/mol) than for alkoxide backbiting (10-15 kcal/mol, except for

trans-CPC). These values are in general agreement with experimental numbers ($E_a = 11 - 19$ kcal/mol),⁹⁵ and they are significantly lower than chromium-bound 32 and 25 kcal/mol for carbonate⁹³ and alkoxide backbiting to give cyclohexene carbonate,⁹⁴ as experimentally observed.

Carbonate backbiting is understood to be S_N2 -type, whereas alkoxide backbiting would be similar to what organic chemists refer to as the $B_{AC}2$ mechanism.⁹⁸ In this mechanism (**Scheme 6**), the alkoxide attacks the carbonate carbon to generate a tetrahedral intermediate. The tetrahedral intermediate either reverts to give polymeric alkoxide, or proceeds to eliminate a cyclic carbonate molecule, and a shortened polymer chain. Due to free alkoxides' affinity for carbon dioxide,⁹⁹ carbonate backbiting proceeds under high- CO_2 conditions, whereas alkoxide backbiting can proceed under low- CO_2 conditions.



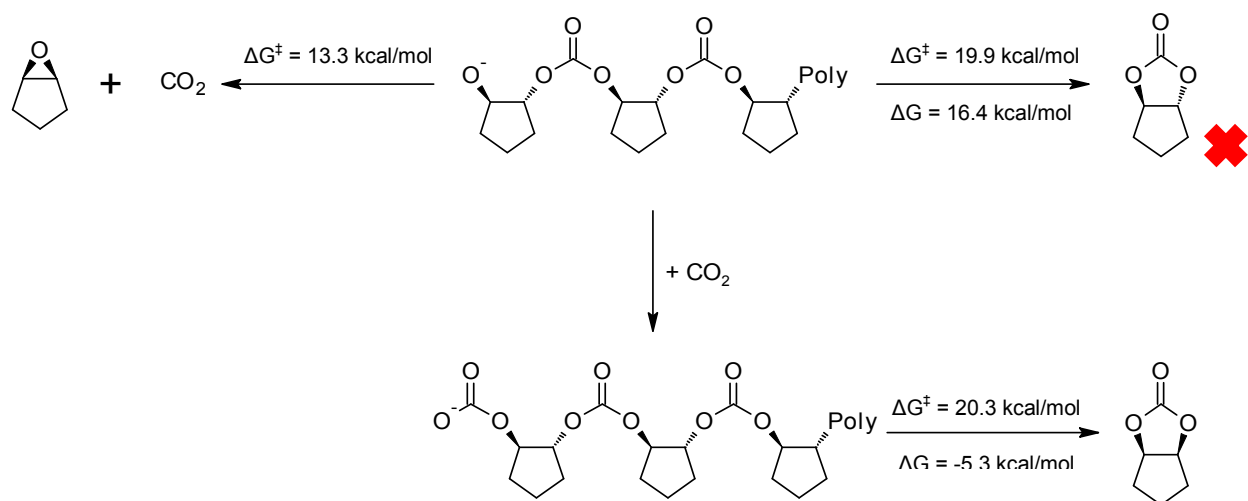
Scheme 6. Mechanism for alkoxide backbiting.

Other significant findings include:

1. Relaxed-chair poly(cyclohexane carbonate) requires an endergonic (+4.7 kcal/mol) conformational change to adopt the boat conformation required for carbonate backbiting. This explains poly(cyclohexane carbonate) tendency not to backbite. In contrast, benzannulated poly(1,4-dihydronaphthalene carbonate) requires no such conformational change, and cyclic carbonate is observed as a side-product.¹⁰⁰
2. Poly(styrene carbonate)'s easy degradation is explained: the transition state for carbonate backbiting is stabilized by resonance with the phenyl group's p_π orbitals, while the

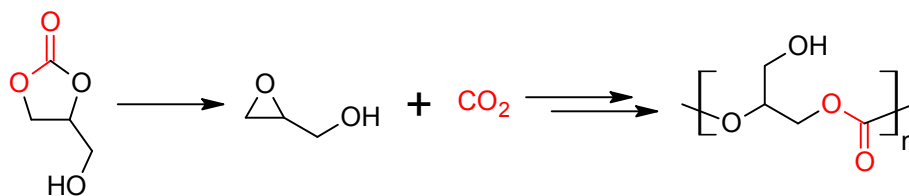
intermediate for alkoxide backbiting is destabilized anti-bonding interactions involving the same.

3. Formation of *trans*-cyclopentene carbonate is exceptionally difficult due to angle strain. Degradation to the epoxide plus carbon dioxide is surprisingly the preferred option as a result (**Scheme 7**), especially where CO₂ is removed to shift the equilibrium toward the polymeric alkoxide.^{67, 68}



Scheme 7. The possible degradation routes available for poly(*trans*-cyclopentene carbonate). Free energy barriers are noted.

The base- and acid-catalyzed decarboxylation reactions of 1,2-glycerol carbonate to yield glycidol that may react with CO₂ to give poly(1,2-glycerol carbonate) were also studied.⁶² Glycerol carbonate may be prepared from glycerol and CO₂, and the polymer is of interest because it represents the conversion of two waste streams into useful products (**Scheme 8**). The authors studied the decarboxylation reactions using CBS-QB3(+), and found that both base- and acid-catalyzed routes are feasible ($\Delta G^\ddagger = 21.7$ and 12.3 kcal/mol , respectively). Future calculations of this nature may need to take into account how B3LYP (used in the CBS-QB3(+) sequence of calculations) tends to overestimate O-C bond lengths in protonated epoxides by 0.2 \AA .¹⁰¹



Scheme 8. 1,2-Glycerol carbonate is decarboxylated to glycidol. After suitable protection, it copolymerizes with CO₂, and poly(1,2-glycerol carbonate) is obtained after deprotection.^{34, 35, 102-108} In this idealized scheme, glycidol copolymerizes with CO₂ that is produced by decarboxylation.

Cyclic carbonate formation

For polymer chemists, cyclic carbonates are usually thought of as unwanted byproducts arising from the metal-bound or metal-free backbiting reactions.⁹⁴ However, these compounds are synthetic targets in their own right, useful as battery electrolytes and as high temperature solvents.^{109, 110} As one of the most exciting advancements in this field, North and coworkers demonstrated a catalytic system that converts ethylene and propylene oxides into the cyclic carbonates using power station flue gas as the carbon dioxide source.⁵

Computational chemistry allows the uncatalyzed reaction between carbon dioxide and epoxide (that normally does not occur) to be studied, providing a point of comparison for catalyzed coupling reactions. In the uncatalyzed reaction, the epoxide oxygen attacks carbon dioxide's central carbon atom, while one of its oxygen atoms attacks the carbon atom forming the base of the epoxide. This is a concerted cycloaddition reaction: two bonds are made, while two bonds are broken, all at the same time. The barrier for this sort of reaction is extremely high: ΔE^\ddagger is ca. 53 and 58 kcal/mol for the reaction between propylene oxide and CO₂ (Figure 6).¹¹¹⁻¹¹⁴

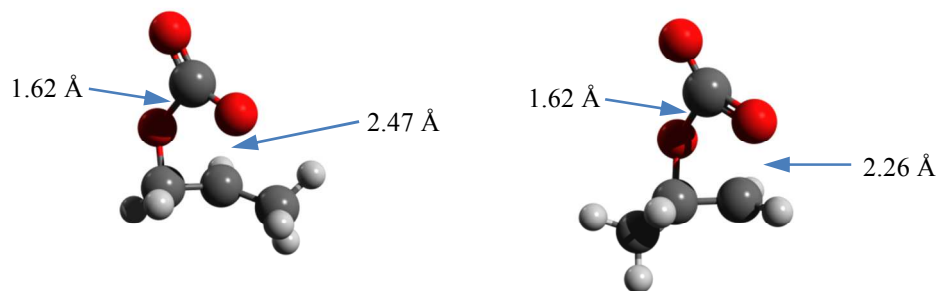


Figure 6. Transition states for the reaction between propylene oxide and carbon dioxide (B3PW91/6-31G(d,p)). The forming O-C bond occurs at the methine position (left) and the methylene position (right).

In the more commonly discussed mechanism of cyclic carbonation formation, the epoxide is attacked by a suitable nucleophile to give an alkoxide that is usually stabilized by some sort of Lewis acid. CO₂ inserts to yield a carbonate that backbites to eliminate the initial nucleophile. This mechanism is akin to the metal-bound or metal-free carbonate backbiting reactions studied by polymer chemists. Lewis acid catalysts for this reaction that have been probed by computational chemistry include: lithium bromide,¹¹⁵ potassium iodide,¹¹³ azolium¹¹¹ and quaternary ammonium salts.^{116, 117} The counterions are not mere spectators; they serve to ring-open the epoxides. The mechanisms for (salphen)Zn and (amino-tris(phenolato))aluminum complexes to catalyze the formation of cyclic carbonates are similar to that discussed in the preceding section (no CO₂ pre-coordination).^{114, 118}

The metal center need not merely serve as a Lewis acid. With cyanomethylcopper(I) as a catalyst, CO₂ inserts into the Cu-CH₂CN bond, serving as a reservoir of activated carbon dioxide.¹¹² Chen, Liu, He *et al.* looked at a cobalt-substituted phosphotungstate catalyst, where activity occurs at the cobalt(II) site.¹¹⁹ Upon coordination, the epoxide is reduced by one electron (generating Co(III)). Homolysis of the epoxide O-C bond produces a carbon radical that reacts with CO₂. Reaction barriers were similar for both doublet and quartet spin states, but the radical mechanism was confirmed experimentally by loss of activity following addition of free radical scavengers. The reaction between Co(II) and CO₂ to give a metallalformate (once postulated by

Paddock and Nguyen¹²⁰) was also ruled out: CO₂ adds to the Co-O bond, generating a four-membered carbonate chelate ring that does not react further.

Re(CO)₅Br is a pro-catalyst for making cyclic carbonates. Wu *et al.* studied two proposed mechanisms for cyclic carbonate formation.¹²¹ The first invokes the oxidative addition of the epoxide O-C bond to the reduced Re(I) center. CO₂ insertion is followed by reductive elimination of the cyclic carbonate. The second mechanism involves insertion of CO₂ into the Re-Br bond. Epoxide binds, and is ring-opened by the activated CO₂ moiety. Rearrangement ensues to generate the cyclic carbonate. The first step of this second mechanism is similar to what Hazari, Kemp, *et al.* have discussed for their chemistry (CO₂ inserting into a Pd-H bond, serving as activated CO₂ for further reaction).¹²² With that said, Wu *et al.* dismissed the second route as unfeasible due to the difficulty of CO₂ insertion into the Re-Br bond. This is consistent with metal-halide bonds being stronger than metal-hydride bonds, CO₂ insertion/deinsertion into the latter generally being thought of as low energy processes.

Concluding remarks

Summarizing the work done to-date, the CBS-4M composite method designed for high accuracy thermochemistry has successfully been used to evaluate the thermodynamics of polycarbonate vs. cyclic carbonate. In the articles reviewed, the enthalpy of the 1-mer to 2-mer reaction adequately represents that of subsequent chain extensions. Other composite methods or high level *ab initio* calculations should, in principle, give equally good results, but they may require too much computer resources for routine use.

Differential functional theory has not been shown to give such chemically-accurate results, but the m06 and m06-2X functionals with triple-zeta basis sets give energies that bracket those obtained by high-level CCSD(T) calculations. The BP86 and the m06-L functionals lacking Hartree-Fock exchange did not do well. The semi-empirical PM6 method is not appropriate for this work, and agreement with experimental enthalpies is fortuitous. The use of periodic boundary conditions should reduce the difficulty of calculation, but the ability to perform DFT frequency calculations under PBC conditions is not widely implemented at this time.

To model the large metal-containing catalytic systems for CO₂-epoxide copolymerization, compromises are necessary. Early studies made use of two-layer ONIOM models with a semi-

empirical low level and a DFT high level. Others analyzed skeletal toy systems using DFT. Reflecting the better computational resources available today, recent investigations have made use of lightly-truncated or non-truncated catalyst models. Calculations performed for selected examples help justify such simplifications.

“Double-barreled” calculations utilizing geometries obtained at lower levels of theory and single point calculations at higher levels of theory have been used. DFT calculations should give qualitatively correct results, although energies obtained differently should be compared with caution. Some authors emphasize the importance of addressing non-covalent interactions to get reliable results (e.g. the dispersion-corrected ω B97X-D functional with basis sets containing diffuse functions). Per common wisdom, the use of a solvation model is helpful, and energetics are overestimated in its absence. Zinc complexes may be assumed to be low-spin singlets, but the lowest energy electronic state for other transition metal complexes should be verified.

The search for better catalysts and more useful polycarbonates continues. Our work with poly(cyclopentene carbonate) has shown beneficial synergism between experimental and computational chemistry: Computational chemistry is used to understand experimental observations. Quantifying reaction energetics in turn allows better-designed experiments, and the pace of research is accelerated as a result. Pertaining to computational chemistry, several aspects of the CO₂-epoxide copolymerization have been explored: the thermodynamics of the process; the kinetics of the zinc-, cobalt-, and chromium-catalyzed chain-extension reactions; the metal-free degradation reactions. Building upon this foundation, we hope to see more successful reports of rational catalyst design in coming years, and overall progress in the field of CO₂ utilization for polymer synthesis.

ACKNOWLEDGEMENT

We gratefully acknowledge the financial support of the National Science Foundation (CHE-1057743) and the Robert A. Welch Foundation (A-0923).

REFERENCES

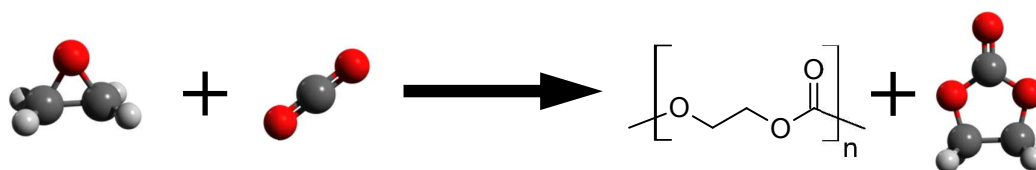
1. DOE/NETL Carbon Dioxide Capture and Storage RD&D Roadmap, http://www.netl.doe.gov/technologies/carbon_seq/refshelf/CCSRoadmap.pdf, 2010.
2. CO₂ Utilization Focus Area, <http://www.netl.doe.gov/research/coal/carbon-storage/research-and-development/co2-utilization>, Accessed 2014-02-10.
3. N. von der Assen, J. Jung and A. Bardow, *Energy Environ. Sci.*, 2013, **6**, 2721.
4. I. S. Metcalfe, M. North, R. Pasquale and A. Thursfield, *Energy Environ. Sci.*, 2010, **3**, 212.
5. M. North, B. Wang and C. Young, *Energy Environ. Sci.*, 2011, **4**, 4163.
6. S. Inoue, H. Koinuma and T. Tsuruta, *J. Polym. Sci., Part B: Polym. Lett.*, 1969, **7**, 287.
7. E. Materials, <http://www.empowermaterials.com/>.
8. Novomer, <http://www.novomer.com/>.
9. Bayer MaterialScience, *Turning Dreams into Value*, <http://www.news.bayer.com/baynews/baynews.nsf/id/98UBA6-Turning-dreams-into-value>, 2013.
10. D. J. Darensbourg and M. W. Holtcamp, *Coord. Chem. Rev.*, 1996, **153**, 155.
11. G. W. Coates and D. R. Moore, *Angew. Chem., Int. Ed.*, 2004, **43**, 6618.
12. H. Sugimoto and S. Inoue, *J. Polym. Sci., Part A: Polym. Chem.*, 2004, **42**, 5561.
13. D. J. Darensbourg, R. M. Mackiewicz, A. L. Phelps and D. R. Billodeaux, *Acc. Chem. Res.*, 2004, **37**, 836.
14. M. H. Chisholm and Z. Zhou, *J. Mater. Chem.*, 2004, **14**, 3081.
15. D. J. Darensbourg, *Chem. Rev.*, 2007, **107**, 2388.
16. S. Klaus, M. W. Lehenmeier, C. E. Anderson and B. Rieger, *Coord. Chem. Rev.*, 2011, **255**, 1460.
17. M. R. Kember, A. Buchard and C. K. Williams, *Chem. Commun.*, 2011, **47**, 141.
18. X. B. Lu and D. J. Darensbourg, *Chem. Soc. Rev.*, 2012, **41**, 1462.
19. D. J. Darensbourg and S. J. Wilson, *Green Chem.*, 2012, **14**, 2665.
20. X.-B. Lu, W.-M. Ren and G.-P. Wu, *Acc. Chem. Res.*, 2012, **45**, 1721.
21. D. J. Darensbourg and M. W. Holtcamp, *Macromolecules*, 1995, **28**, 7577.
22. D. J. Darensbourg, M. W. Holtcamp, G. E. Struck, M. S. Zimmer, S. A. Niezgodna, P. Rainey, J. B. Robertson, J. D. Draper and J. H. Reibenspies, *J. Am. Chem. Soc.*, 1999, **121**, 107.
23. D. R. Moore, M. Cheng, E. B. Lobkovsky and G. W. Coates, *J. Am. Chem. Soc.*, 2003, **125**, 11911.
24. F. Jutz, A. Buchard, M. R. Kember, S. B. Fredriksen and C. K. Williams, *J. Am. Chem. Soc.*, 2011, **133**, 17395.
25. K. B. Hansen, J. L. Leighton and E. N. Jacobsen, *J. Am. Chem. Soc.*, 1996, **118**, 10924.
26. R. M. Thomas, P. C. B. Widger, S. M. Ahmed, R. C. Jeske, W. Hirahata, E. B. Lobkovsky and G. W. Coates, *J. Am. Chem. Soc.*, 2010, **132**, 16520.
27. P. C. Widger, S. M. Ahmed, W. Hirahata, R. M. Thomas, E. B. Lobkovsky and G. W. Coates, *Chem. Commun.*, 2010, **46**, 2935.
28. S. M. Ahmed, A. Poater, M. I. Childers, P. C. Widger, A. M. LaPointe, E. B. Lobkovsky, G. W. Coates and L. Cavallo, *J. Am. Chem. Soc.*, 2013, **135**, 18901.
29. D. J. Darensbourg and S. J. Wilson, *J. Am. Chem. Soc.*, 2011, **133**, 18610.
30. D. J. Darensbourg and S. J. Wilson, *Macromolecules*, 2013, **46**, 5929.

31. C. M. Byrne, S. D. Allen, E. B. Lobkovsky and G. W. Coates, *J. Am. Chem. Soc.*, 2004, **126**, 11404.
32. M. O. Sonnati, S. Amigoni, E. P. Taffin de Givenchy, T. Darmanin, O. Choulet and F. Guittard, *Green Chem.*, 2013, **15**, 283.
33. J. R. Ochoa-Gómez, O. Gómez-Jiménez-Aberasturi, C. Ramírez-López and M. Belsué, *Org. Process Res. Dev.*, 2012, **16**, 389.
34. H. Zhang and M. W. Grinstaff, *J. Am. Chem. Soc.*, 2013, **135**, 6806.
35. J. Geschwind and H. Frey, *Macromolecules*, 2013, **46**, 3280.
36. Z. Liu, M. Torrent and K. Morokuma, *Organometallics*, 2002, **21**, 1056.
37. M. Drees, M. Cokoja and F. E. Kühn, *ChemCatChem*, 2012, **4**, 1703.
38. T. Fan, X. Chen and Z. Lin, *Chem. Commun.*, 2012, **48**, 10808.
39. M. D. Dadmun, *Computational Studies, Nanotechnology, and Solution Thermodynamics of Polymer Systems*, Kluwer Academic/Plenum Publishers, New York, 2001.
40. M. P. Stevens, *Polymer Chemistry: An Introduction*, Oxford University Press, New York, 1999.
41. A. Duda and A. Kowalski, in *Handbook of Ring-Opening Polymerization*, Wiley-VCH Verlag GmbH & Co. KGaA, 2009, pp. 1-51.
42. A. L. L. East, in *Encyclopedia of Computational Chemistry*, John Wiley & Sons, Ltd, 2002.
43. F. S. Dainton and K. J. Ivin, *Q. Rev. Chem. Soc.*, 1958, **12**, 61.
44. S. J. Blanksby and G. B. Ellison, *Acc. Chem. Res.*, 2003, **36**, 255.
45. S. W. Benson, *J. Chem. Educ.*, 1965, **42**, 502.
46. S. W. Benson and J. H. Buss, *J. Chem. Phys.*, 1958, **29**, 546.
47. S. W. Benson, F. R. Cruickshank, D. M. Golden, G. R. Haugen, H. E. O'Neal, A. S. Rodgers, R. Shaw and R. Walsh, *Chem. Rev.*, 1969, **69**, 279.
48. N. Cohen and S. W. Benson, *Chem. Rev.*, 1993, **93**, 2419.
49. C. J. Price, B. J. E. Reich and S. A. Miller, *Macromolecules*, 2006, **39**, 2751.
50. D. J. Darensbourg and A. D. Yeung, *Macromolecules*, 2013, **46**, 83.
51. E. N. Brothers, A. F. Izmaylov, A. A. Rusakov and G. E. Scuseria, *J. Phys. Chem. B*, 2007, **111**, 13869.
52. A. Kržan, *J. Mol. Struct. Theochem*, 2009, **902**, 49.
53. J. M. Goodman, *J. Chem. Inf. Model.*, 1997, **37**, 876.
54. N. O. Luttschwager, T. N. Wassermann, R. A. Mata and M. A. Suhm, *Angew. Chem., Int. Ed. Engl.*, 2013, **52**, 463.
55. J. N. Byrd, R. J. Bartlett and J. A. Montgomery, *J. Phys. Chem. A*, 2014, doi: 10.1021/jp4121854.
56. M. W. Lehenmeier, C. Bruckmeier, S. Klaus, J. E. Dengler, P. Deglmann, A. K. Ott and B. Rieger, *Chem. Eur. J.*, 2011, **17**, 8858.
57. A. D. Yeung, Ph.D. Dissertation, Texas A&M University, 2014.
58. E. G. Lewars, *Computational Chemistry*, Springer Netherlands, 2011.
59. A. F. Kazakov, C. D. Muzny, R. D. Chirico, V. Diky and M. Frenkel, *NIST/TRC Web Thermo Tables - Professional Edition NIST Standard Reference Subscription Database 3*, Thermodynamics Research Center, Boulder, CO, 2002.
60. P. J. Linstrom and W. G. Mallard, *NIST Standard Reference Database Number 69*, National Institute of Standards and Technology, Gaithersburg, MD, 2005.

61. H.-Y. Chen, J. Zhang, C.-C. Lin, J. H. Reibenspies and S. A. Miller, *Green Chem.*, 2007, **9**, 1038.
62. D. J. Darensbourg and A. D. Yeung, *Green Chem.*, 2014, **16**, 247.
63. D. J. Darensbourg and A. I. Moncada, *Macromolecules*, 2009, **42**, 4063.
64. T. Ariga, T. Takata and T. Endo, *Macromolecules*, 1997, **30**, 737.
65. H. R. Kricheldorf and B. Weegen-Schulz, *Macromolecules*, 1993, **26**, 5991.
66. H. R. Kricheldorf and B. Weegen-Schulz, *Polymer*, 1995, **36**, 4997.
67. D. J. Darensbourg, A. D. Yeung and S.-H. Wei, *Green Chem.*, 2013, **15**, 1578.
68. D. J. Darensbourg, S.-H. Wei, A. D. Yeung and W. C. Ellis, *Macromolecules*, 2013, **46**, 5850.
69. E. L. Marshall, V. C. Gibson and H. S. Rzepa, *J. Am. Chem. Soc.*, 2005, **127**, 6048.
70. A. P. Dove, V. C. Gibson, E. L. Marshall, H. S. Rzepa, A. J. P. White and D. J. Williams, *J. Am. Chem. Soc.*, 2006, **128**, 9834.
71. L. Wang, C. E. Kefalidis, S. Sinbandhit, V. Dorcet, J. F. Carpentier, L. Maron and Y. Sarazin, *Chem. - Eur. J.*, 2013, **19**, 13463.
72. M. O. Miranda, Y. DePorre, H. Vazquez-Lima, M. A. Johnson, D. J. Marell, C. J. Cramer and W. B. Tolman, *Inorg. Chem.*, 2013, **52**, 13692.
73. M. W. Lehenmeier, S. Kissling, P. T. Altenbuchner, C. Bruckmeier, P. Deglmann, A. K. Brym and B. Rieger, *Angew. Chem., Int. Ed. Engl.*, 2013, **52**, 9821.
74. A. Buchard, F. Jutz, M. R. Kember, A. J. P. White, H. S. Rzepa and C. K. Williams, *Macromolecules*, 2012, **45**, 6781.
75. J. D. Chai and M. Head-Gordon, *Phys. Chem. Chem. Phys.*, 2008, **10**, 6615.
76. X. Pan, Z. Liu, R. Cheng, D. Jin, X. He and B. Liu, *J. Organomet. Chem.*, 2014, **753**, 63.
77. G. A. Luinstra and F. Molnar, *Macromol. Symp.*, 2007, **259**, 203.
78. *US Pat.*, 4943677 A, 1990.
79. E. N. Jacobsen, *Acc. Chem. Res.*, 2000, **33**, 421.
80. K. Sun, W.-X. Li, Z. Feng and C. Li, *Chem. Phys. Lett.*, 2009, **470**, 259.
81. D. D. Ford, L. P. Nielsen, S. J. Zuend, C. B. Musgrave and E. N. Jacobsen, *J. Am. Chem. Soc.*, 2013, **135**, 15595.
82. P. G. Cozzi, *Chem. Soc. Rev.*, 2004, **33**, 410.
83. J. Fang, A. Walshe, L. Maron and R. J. Baker, *Inorg. Chem.*, 2012, **51**, 9132.
84. M. C. Curet-Arana, P. Meza, R. Irizarry and R. Soler, *Top. Catal.*, 2012, **55**, 260.
85. D. J. Darensbourg, A. Rokicki and M. Y. Darensbourg, *J. Am. Chem. Soc.*, 1981, **103**, 3223.
86. D. J. Darensbourg and A. Rokicki, *Organometallics*, 1982, **1**, 1685.
87. D. J. Darensbourg, R. K. Hanckel, C. G. Bauch, M. Pala, D. Simmons and J. N. White, *J. Am. Chem. Soc.*, 1985, **107**, 7463.
88. D. J. Darensbourg and G. Grottsch, *J. Am. Chem. Soc.*, 1985, **107**, 7473.
89. D. J. Darensbourg, P. Wiegrefe and C. G. Riordan, *J. Am. Chem. Soc.*, 1990, **112**, 5759.
90. D. J. Darensbourg, H. P. Wiegrefe and P. W. Wiegrefe, *J. Am. Chem. Soc.*, 1990, **112**, 9252.
91. D. Adhikari, S. T. Nguyen and M. H. Baik, *Chem. Commun.*, 2014, **50**, 2676.
92. S. J. Na, S. S. A. Cyriac, B. E. Kim, J. Yoo, Y. K. Kang, S. J. Han, C. Lee and B. Y. Lee, *Inorg. Chem.*, 2009, **48**, 10455.
93. D. J. Darensbourg, J. C. Yarbrough, C. Ortiz and C. C. Fang, *J. Am. Chem. Soc.*, 2003, **125**, 7586.

94. D. J. Darensbourg, P. Bottarelli and J. R. Andreatta, *Macromolecules*, 2007, **40**, 7727.
95. D. J. Darensbourg and S.-H. Wei, *Macromolecules*, 2012, **45**, 5916.
96. G. A. Luinstra, G. R. Haas, F. Molnar, V. Bernhart, R. Eberhardt and B. Rieger, *Chem. Eur. J.*, 2005, **11**, 6298.
97. S. Parthiban, G. de Oliveira and J. M. L. Martin, *J. Phys. Chem. A*, 2001, **105**, 895.
98. R. Bruckner, *Advanced Organic Chemistry - Reaction Mechanisms*, Harcourt/Academic Press, San Diego, 2002.
99. B. O. Heston, O. C. Dermer and J. A. Woodside, *Proc. Okl. Acad. Sci.*, 1942, **23**, 67.
100. D. J. Darensbourg, S. J. Kyran and A. D. Yeung, *In preparation*, 2014.
101. Y. Zhao and D. G. Truhlar, *J. Org. Chem.*, 2006, **72**, 295.
102. J. Hilf and H. Frey, *Macromol. Rapid Commun.*, 2013, **34**, 1395.
103. J. Łukaszczyk, K. Jaszcz, W. Kuran and T. Listoś, *Macromol. Biosci.*, 2001, **1**, 282.
104. Q. Zhou, L. Gu, Y. Gao, Y. Qin, X. Wang and F. Wang, *J. Polym. Sci., Part A: Polym. Chem.*, 2013, **51**, 1893.
105. N.-Y. Mun, K.-H. Kim, D.-W. Park, Y. Choe and I. Kim, *Korean J. Chem. Eng.*, 2005, **22**, 556.
106. W.-M. Ren, M.-W. Liang, Y.-C. Xu and X.-B. Lu, *Polym. Chem.*, 2013, **4**, 4425.
107. J. Geschwind and H. Frey, *Macromol. Rapid Commun.*, 2013, **34**, 150.
108. J. Hilf, A. Phillips and H. Frey, *Polym. Chem.*, 2014, **5**, 814.
109. M. North, R. Pasquale and C. Young, *Green Chem.*, 2010, **12**, 1514.
110. A. Decortes, A. M. Castilla and A. W. Kleij, *Angew. Chem., Int. Ed. Engl.*, 2010, **49**, 9822.
111. H. Sun and D. Zhang, *J. Phys. Chem. A*, 2007, **111**, 8036.
112. C. H. Guo, H. S. Wu, X. M. Zhang, J. Y. Song and X. Zhang, *J. Phys. Chem. A*, 2009, **113**, 6710.
113. J. Ma, J. Liu, Z. Zhang and B. Han, *Green Chem.*, 2012, **14**, 2410.
114. F. Castro-Gomez, G. Salassa, A. W. Kleij and C. Bo, *Chem. - Eur. J.*, 2013, **19**, 6289.
115. Y. Ren, C.-H. Guo, J.-F. Jia and H.-S. Wu, *J. Phys. Chem. A*, 2011, **115**, 2258.
116. J.-Q. Wang, K. Dong, W.-G. Cheng, J. Sun and S.-J. Zhang, *Catal. Sci. Tech.*, 2012, **2**, 1480.
117. S. Foltran, R. Mereau and T. Tassaing, *Catal. Sci. Tech.*, 2014.
118. C. J. Whiteoak, N. Kielland, V. Laserna, F. Castro-Gomez, E. Martin, E. C. Escudero-Adan, C. Bo and A. W. Kleij, *Chemistry*, 2014, **20**, 2264.
119. F. Chen, X. Li, B. Wang, T. Xu, S. L. Chen, P. Liu and C. Hu, *Chemistry*, 2012, **18**, 9870.
120. R. L. Paddock and S. T. Nguyen, *J. Am. Chem. Soc.*, 2001, **123**, 11498.
121. C.-H. Guo, J.-Y. Song, J.-F. Jia, X.-M. Zhang and H.-S. Wu, *Organometallics*, 2010, **29**, 2069.
122. H.-W. Suh, T. J. Schmeier, N. Hazari, R. A. Kemp and M. K. Takase, *Organometallics*, 2012, **31**, 8225.

Graphical Abstract

**Computational chemistry:**

Thermodynamics of copolymerization
Kinetics of chain growth and degradation
Experimental-computational synergism
Rational catalyst design?